Composite Structures 312 (2023) 116861

Contents lists available at ScienceDirect

Composite Structures

journal homepage: www.elsevier.com/locate/compstruct

A novel multi-scale modelling approach to predict the reduction of transverse strength due to porosity in composite materials

Benjamin Fisher *, Mark Eaton, Rhys Pullin

Cardiff School of Engineering, Queen's Buildings, Cardiff University, 5 The Parade, Newport Road, Cardiff CF24 3AA, United Kingdom

ARTICLE INFO

Keywords:
Multi-scale modelling
Porosity/voids
Empirical testing

ABSTRACT

Porosity is a major manufacturing defect which affects the matrix dominate properties of continuous fibre composites, in particular the transverse strength. The simulation of porosity allows for predictions on the reduction of strength to be made, however, there is a trade-off between accuracy and computational efficiency. The multi-scale modelling approach presented here allows for accurate 3-dimensional geometry data of voids to be used. This is accomplished by first evaluating the effect the porosity has on degrading the matrix then subsequently, by using a representative unit cell, ply level strength can be predicted. The model is validated against empirical tensile and compressive testing of unidirectional autoclave cured prepreg with strong correlation. The approach allows for a reduction in overengineered structures by predicting accurate material properties for a given porosity generation.

1. Introduction

The automotive industry is under pressure to improve the environmental impact with the main cause for concern being the carbon footprint left behind due to Internal Combustion Engines (ICE), particularly since the number of vehicles is increasing each year[1,2]. Whilst significant research is put into improving the efficiency of the ICE[3] and development of electric drivetrains shows promising progress[4], both situations must be accompanied by vehicle lightweighting. Carbon Fibre Reinforced Plastics (CFRP) is gaining significant traction in the automotive industry as it offers potential for lightweighting without penalty to the mechanical performance[5,6].

The complex nature of CFRP means that there is a wide array of defects that can occur during the manufacturing stage[7,8] leading to uncertainty in designs[9]. For this reason, whilst composite structures can be found on high performance/low volume vehicles, often, production vehicles limit the usage of CFRP to, when used, non-structural purposes[6]. This is since it is crucial to have certainty in understanding the behaviour of load bearing structures and although high safety factors could be used to pass safety requirements, this detracts from the philosophy of lightweighting[10]. For load bearing usage of CFRP within production vehicles to become more commonplace, significant research has been invested into understanding how these defects generate during manufacture as well as understanding the impact on mechanical performance[11]. For the purpose of this paper, only the impact porosity has on mechanical performance is investigated.

The impact on mechanical performance due to porosity has been extensively studied experimentally and results have shown that voids predominately affect matrix-based properties, including compression, transverse tension and Interlaminar Shear Strength (ILSS). An early study by Olivier et al.[12] showed that whilst transverse tensile modulus and strength were both significantly affected by voids, the longitudinal modulus remained unaffected with only a slight drop in strength. More recently Zhang et al.[13] increased the porosity from 0.33 % to 1.50 % in quasi-isotropic laminates and found a reduction in tensile strength by up to 2.36 %. Similarly Li et al.[14] found an increase in porosity from 0.7 % to 5.4 % led to a reduction in tensile strength of 15.3 % and tensile modulus by 12.6 %. Stamopoulos et al.[15] manufactured laminates with void fractions ranging from 0.82 % to 3.4 % and found that whilst all measured properties were affected by voids, strength properties were most affected, with flexural strength being the worst affected at 16.6 % reduction in strength. Liu et al.[16] also found that flexural strength was significantly affected by increasing void content as well as the ILSS and tensile strength. Costa et al.[17] studied the ILSS in two different resin systems where both results showed a decrease in ILSS as porosity increases, whilst Landro et al.[18] reported a 25 % decrease in short beam shear strength at 6.6 % voids.

From these studies it is clear porosity has a significant impact on the

* Corresponding author.
E-mail address: fisherb2@cardiff.ac.uk (B. Fisher).

https://doi.org/10.1016/j.compstruct.2023.116861
Received 9 June 2022; Received in revised form 16 February 2023; Accepted 25 February 2023
Available online 2 March 2023

mechanical properties of composites, particularly for matrix-based properties. Due to the complexity of how voids form and the wide array of parameters that can be impacted, research is still ongoing. Although material properties can be directly measured from empirical testing it is often very difficult to isolate one variable at a micro-mechanics scale. For this reason, microscale computational modelling is often used to study the effects of porosity as it allows individual factors to be changed independently. The major drawback, however, is finding the balance between realistic geometry that accurately describes the assembly of fibres, matrix and voids and a model that can solve in an appropriate amount of time. There are two major approaches commonly used, either a 2D analysis where voids are modelled as cavities in the unit cell[19–22], or a 3D analysis where elements are used to represent voids[23–25]. The two approaches are discussed in further detail as follows.

A 2D unit cell comprising of a uniform array of fibres was modelled by Nikopour[19] to study the effect on the transverse elastic properties between models with and without voids. This is an idealistic assumption since fibres and voids are randomly distributed[26]. These simplifications were addressed by Dong[20] where the constituents were randomly distributed in the unit cell. Dong also investigated the impact on composite strength as well as elastic properties. Li et al.[21] produced similar models, however, void distribution was based on microscopy with their results showing that the distribution did not affect strength and stiffness. The 2D unit cells described so far only consider microvoids, small circular voids that occur between fibres, in contrast Ashouri Vajari et al.[22] developed a model which also accounted for larger interfibre voids. The approach accounted for both matrix and fibre–matrix failure and showed that the interfibre voids had a significant affect on the strength of the composites and, similar to Li et al.[21], microvoids affected damage progression.

Although 2D approaches have yielded good correlation with either analytical models or experimental testing, the approach does not account for the full three-dimensional shape of the void. Planar models assume voids are infinitely long with constant cross section, however, voids typically have a finite length and are ellipsoidal in shape [15,27,28]. To understand how the 3-dimensional void shape affects elastic properties Huang and Talreja[29] varied void geometry with good correlation against analytical models. Another 3D approach is to reduce the stiffness matrix of randomly selected elements representing them as voids. Huang[23] and Dong[24] successfully accomplished this to study the impact on elasticity due to porosity. Jiang et al[25] had a similar approach and was able to also predict the strength degradation with good corelation to analytical models.

It is clear from the literature that there is a drive towards developing modelling techniques which accounts for accurate void geometry, however, a balance must be found between modelling representative geometry and computational efficiency. 2D simulations provides efficiency but lacks geometrical accuracy. In contrast, 3D analysis simulating voids as elements retains the efficiency and does not assume infinity long voids, however, can only account for micro voids and also void geometry must take the shape of the element.

This paper aims to present an efficient modelling approach, accounting for accurate void geometry, to predict the effective transverse tensile and compressive strength as a result of the porosity. This is achieved through a 2-stage multiscale modelling procedure using void characterisation data. The Stage 1 model investigates how voids act as stress concentrations on pure resin. Load is induced into the model until failure is observed. In this study brittle failure is assumed which is determined when an element fails, i.e., the stress of an element matches the material strength. Whilst brittle failure was assumed for this study, the framework is not limited to this assumption and can be adapted accordingly. At the sufficient load applied for failure to be observed, the global stress of the model is measured (a function of the applied force and model area) and recorded as the degraded/effective matrix strength for the given porosity parameters modelled. The output of this model is in the μm scale length. The effective strength is then used in the Stage 2 model comprising of a Representative Unit Cell (RUC). The same procedure is followed whereby the load is induced until failure is observed, at which point the model strength is calculated (again based on the applied force and model area). The Stage 2 model predicts ply level strengths at the mm scale length, for composite structural design, for the region where the void characterisation measurements were taken. The novelty of this approach is through a combination of modelling 3D void geometry in full, rather than in a planar model or simulated as an element, to predict the transverse strengths as well as splitting the model into the two separate stages. The structure of this paper is such that experimental work is described in Section (2), including void characterisation. The experimental results including discussion in detailed in Section (3). The model framework is outlined in Section (4) and Section (5) details the application of the model using the experimental results as well as the correlation. Lastly, Section (6) provides concluding remarks.

2. Experimental procedure

To understand the magnitude of impact that porosity has and provide useful test data to incorporate into the modelling procedure, experimental testing has been performed. This has involved testing laminates with varying porosity, through adjusting the cure pressure, and characterised through microscopy. The characterisation of voids informs the models created and the mechanical testing data is used to validate the modelling results, as shown in Section 5.

2.1. Void characterisation

To accurately understand how the porosity affects the laminates mechanical properties optical microscopy and image processing was utilised. To prepare for microscopy three 25x15mm samples were cut from each laminate and polished up to 4000 grit using Mirka WPF wet and dry sanding sheets. Inspection was performed using a Leica DM LM microscope with digital images captured by an iDS UI-1460LE-C-HQ camera controlled through a PC running Buehler OmniMet Modular Imaging System (OMIS) software. The images were either processed directly to measure the void dimensions through the OMIS software or to measure the void content a post-processing Python script was used to detect porous regions and subsequently calculate the void content, which is a common approach taken[30,31]. The approach converts the image to greyscale and a threshold is set such that each pixel is set either to black or white based on their greyscale value, where black pixels represent porous regions. Void content is calculated by the ratio between the black to white pixels. To measure the void dimensions a 20x/0.40BD lens was used and focused on 30 individual voids measuring from tip-to-tip in both the longitudinal and transverse direction. In contrast, images for void content analysis were captured using a 10X/0.25BD lens, since this gives a wider field of view whilst retaining definition. 60 images were taken from each sample to ensure accurate representation was captured.

2.2. Materials and specimen preparation

The material used in this study is Skyflex K51 (USN200B) supplied by SK Chemicals. This is an epoxy prepreg containing 15 K Pyrofil TR50S carbon fibres. The properties of the carbon fibres are given in Table 1. Whilst a resin content (by mass) of 33% is specified, the mechanical properties of the epoxy resin used in this prepreg are not disclosed by the supplier. The laminates were cured in an autoclave using a dual temperature dwell (30 min at 80 °C and 90 min at 125 °C) at a constant pressure.

Each laminate was assigned a different cure pressure to vary the porosity of each laminate. The first laminate was subjected to vacuum bag pressure only, set at 0.05 MPa. The remaining samples were cured with autoclave pressures of 0.1, 0.3 and 0.5 MPa, with a vacuum bag

Table 1
Fibre Properties.

Fibre Designation	Filament Count	Filament Diameter	Tensile Strength	Tensile Modulus	Elongation	Density
TR 50S15L	15,000	7 μm	4.12 GPa	235 GPa	2.1%	1.82 g/cm^3

pressure of 0.09 MPa. Laminates with two uniaxial layups, $[90]_8$ and $[90]_{16}$, were manufactured for testing tensile and compressive properties, respectively, resulting in 8 laminates. The specimen and tab geometries were determined based on guidance in ASTM standards D3039 (tension) and D6641 (compression). G10 Epoxy Glass laminate was used as a tabbing material and was first bonded onto the laminate using ET538 2-Part Structural Adhesive, manufactured by Permabond Engineering Adhesives Limited, before cutting the specimens to size. Specimens were polished using a 120 grit abrasive paper to remove the machining marks, and then polished using a 240 grit abrasive paper to the same finish. Examples of each specimen can be seen in Fig. 1.

2.3. Testing procedure and material property evaluation

Tensile testing was preformed using an Instron 8801 servo hydraulic testing machine. Specimens were appropriately aligned and tightening the grips induces in a small preload, this was kept constant across all specimens at 10 Newtons. Load was induced through crosshead displacement using a constant head-speed of 2 mm/min as recommended in the testing standard ASTM D3039.

Compressive testing was preformed using a Combined Loading Compression (CLC) fixture in a ZwickRoell Z050 testing machine following ASTM D6641 testing standards. Specimens were carefully aligned in the test CLC fixture between fixed flat platens such that they were centred appropriately, and the ends were flush with the edges of the fixture. A bolt torque of 3.5Nm provided sufficient clamping force to achieve the correct failure mode. Load was induced through crosshead displacement at a rate of 1.3 mm/min until specimen failure.

For every specimen tested the cross-sectional area was recorded, along with the load, displacement, test time and strain. The cross-sectional area and maximum load were used to calculate the strength of each specimen and the modulus was determined for by measuring the sample strain using iMetrum's video strain gauge system. This comprising of an iMetrum camera, a general-purpose lens for tensile testing and a high magnification material lens for the compression testing. A 60 mm and 8 mm '*virtual*' gauge length was used for the tensile and compressive specimens respectively.

3. Experimental results and discussion

3.1. Void characterisation

The mean of the measured values of void content of each laminate are given in Table 2, along with the error given as a single standard deviation. Generally, as the cure pressure reduces the void content increases as expected. However, in some cases, specifically the tensile laminate cured at 0.39 MPa and compressive laminate cured at 0.59 MPa, this trend was not followed. The error in void content measurement is high, however, this was to be expected due to using microscopy only capturing a smaller area per image. For this reason, a high number of images were taken (60 per laminate) to ensure a representative area was analysed. Since the processed images used to measure the void content clearly show the porosity, they can also provide an insight into the dispersion of the voids. Fig. 2 shows how the voids are typically dispersed. Whilst void dispersion is not perfectly periodic, what is

Table 2
Average void content for each laminate.

Test laminate	Layup	Cure Pressure / MPa	Void Content / %	Standard Deviation / %
Tension	$[90]_8$	0.59	0.63	0.49
		0.39	1.28	1.99
		0.19	0.88	0.93
		0.05	2.01	1.53
Compression	$[90]_{16}$	0.59	0.87	0.61
		0.39	0.66	0.38
		0.19	1.14	1.01
		0.05	1.58	1.08

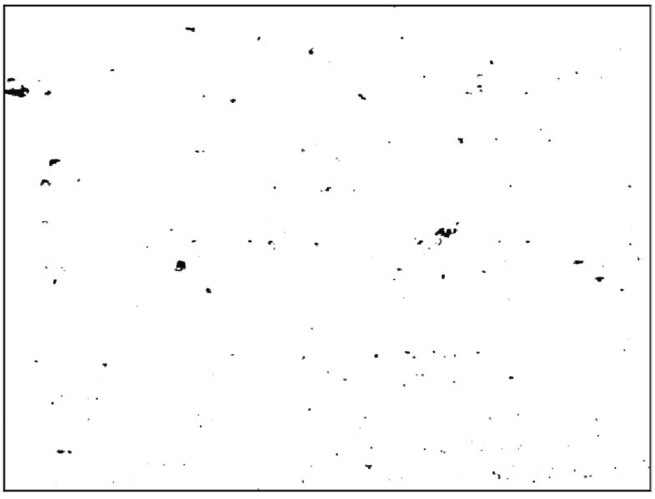

Fig. 2. Typical dispersion of voids throughout the laminates.

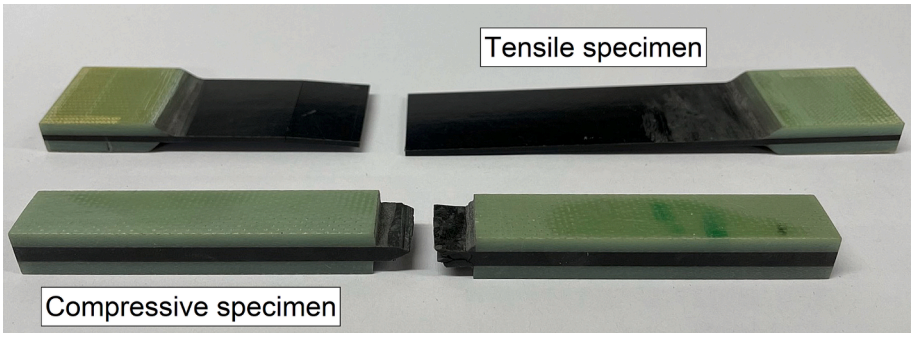

Fig. 1. Typical tensile and compressive specimens. Failure location can be seen in the gauge sections.

evident from the processed images is that, for the most part, the voids are spread evenly. From a modelling perspective, this means that a single void can be modelled with the assumption that it is repeating. This assumption means that high fidelity models which accurately describe the porosity dispersion are not required reducing computation requirements whilst retaining accuracy.

Fig. 3(A) shows an image from the $[90]_{16}$ laminate cured at 0.05 MPa (selected for measurement clarity of larger voids) used to measure void dimensions. From these images the longitudinal and transverse size distributions were determined for each laminate. A general trend of most laminates was found, as represented by Fig. 3(B) for the $[90]_8$ laminate cured at 0.39 MPa, whereby a definitive length of voids in both the longitudinal and transverse directions can be identified by the peak of the distribution. For this specific laminate both the longitudinal and transverse length of most voids are between 4 and 8 μm. Since this shows that most voids are of similar size it further supports the assumption that a single void, representing the mean of all 30 measurements, can be used to model the influence on strength. However, reducing the distribution of measured void sizes to a single void geometry carries some uncertainty. To provide better understanding, the distribution has been represented by a range of statistical parameters which include: The approaches included: Mean-all (mean of all measurements), Mean-StdDev (mean of the measurements within one standard deviation of Mean-all results), Median (middle value of all measurements) and Lower Third (mean of the lower third number of measurements). The comparison of the different approaches is discussed in Section 5.2.

3.2. Experimental testing

The results of how porosity effects the transverse tensile strength and modulus are presented in Fig. 4(A) and (B). This figure contains modelling data (coloured red) which will be discussed in section 5.2. The error bars represent a single standard deviation of the test data. Since the strength and stiffness data was calculated from the same test, the void content and associated error is the same, therefore the void content error for the modulus results has been omitted for clarity. This has also been done for the compression results below. As the overall void content increases there is a reduction in strength from a maximum of 60.40 MPa with a corresponding void content of 0.63% down to a minimum strength of 50.95 MPa with a corresponding void content of 2.01%. This gives an overall reduction in tensile strength of 15.6% for an increase in void content of 1.38%. This is expected as when the void content increased the typical voids size also increased, from an average of ~ 7 μm in the lowest porosity laminate up to an average of ~ 50 μm in the most porous laminate. There appears to be a non-linear trend in strength versus porosity such that strength is more sensitive to changes in porosity at lower void contents and as the void content increases the effect is it has on the knockdown in strength diminishes. This is likely due to the geometry of the voids; at lower porosities the voids are typically smaller meaning that the radius of voids acts as higher stress raisers within the laminate. Whereas larger voids formed at low cure pressure void have larger radii which act as lower stress raisers. In contrast to the effect that porosity has on the tensile strength, as the void content is increased, the modulus remains largely unaffected. This is likely due to the small volume fraction of voids in the laminates, which in the worst case is approximately 2% of the laminate volume. Such a small change in resin content of the laminate is unlikely to create a measurable effect on modulus relative to testing variability/uncertainty.

The results of how porosity affects the transverse compressive strength and modulus are presented in Fig. 4(C) and (D) with the error bars presented as a single standard deviation. The results show a significant reduction in strength as the porosity increases; whilst the transverse strength is 177.9 MPa at a porosity of 0.66%, as the porosity is increased to 1.58% the transverse strength reduces to 154.5 MPa. This is an overall reduction in strength of 13.1% for a 0.92% increase in void content. There appears to be a similar non-linear trend as found from the tensile results, such that the rate at which the strength diminishes is reduced at higher void contents. Again, this is expected to be due to the size of voids found in the laminate and how the shape of the voids act as stress concentrations. Within the lowest void content laminate the average longitudinal length of the voids are approximately 12 μm whereas the average longitudinal length of the voids within the most porous laminate are approximately 26 μm, with the trend following suit for the laminates in between. Whilst having a more porous laminate reduces the strength, since the voids within it are larger the stress concentrations associated with them are lower (due to larger radii) and so the effect is reduced, leading to the non-linear trend. Further analysis and discussion of this effect is given in subsection 5.3. In contrast to the tensile results, there is more of variation in the compressive modulus. Initially, at low void contents, there is a reduction in stiffness, however, at the highest void content the stiffness increases. Further investigations would be required to draw accurate conclusions to whether there is a significant change in modulus due to increasing porosity, however, that is beyond the scope of this study which is focused on the effect of

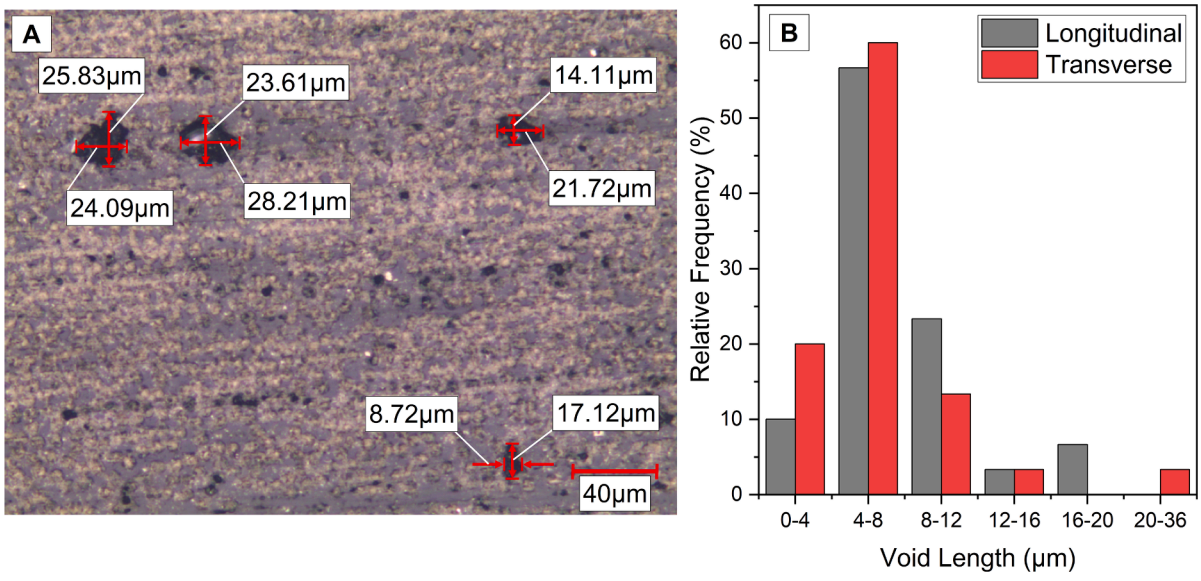

Fig. 3. Dimension of voids within the laminates measured through microscopy (A) and typical histogram of void dimension distribution (B).

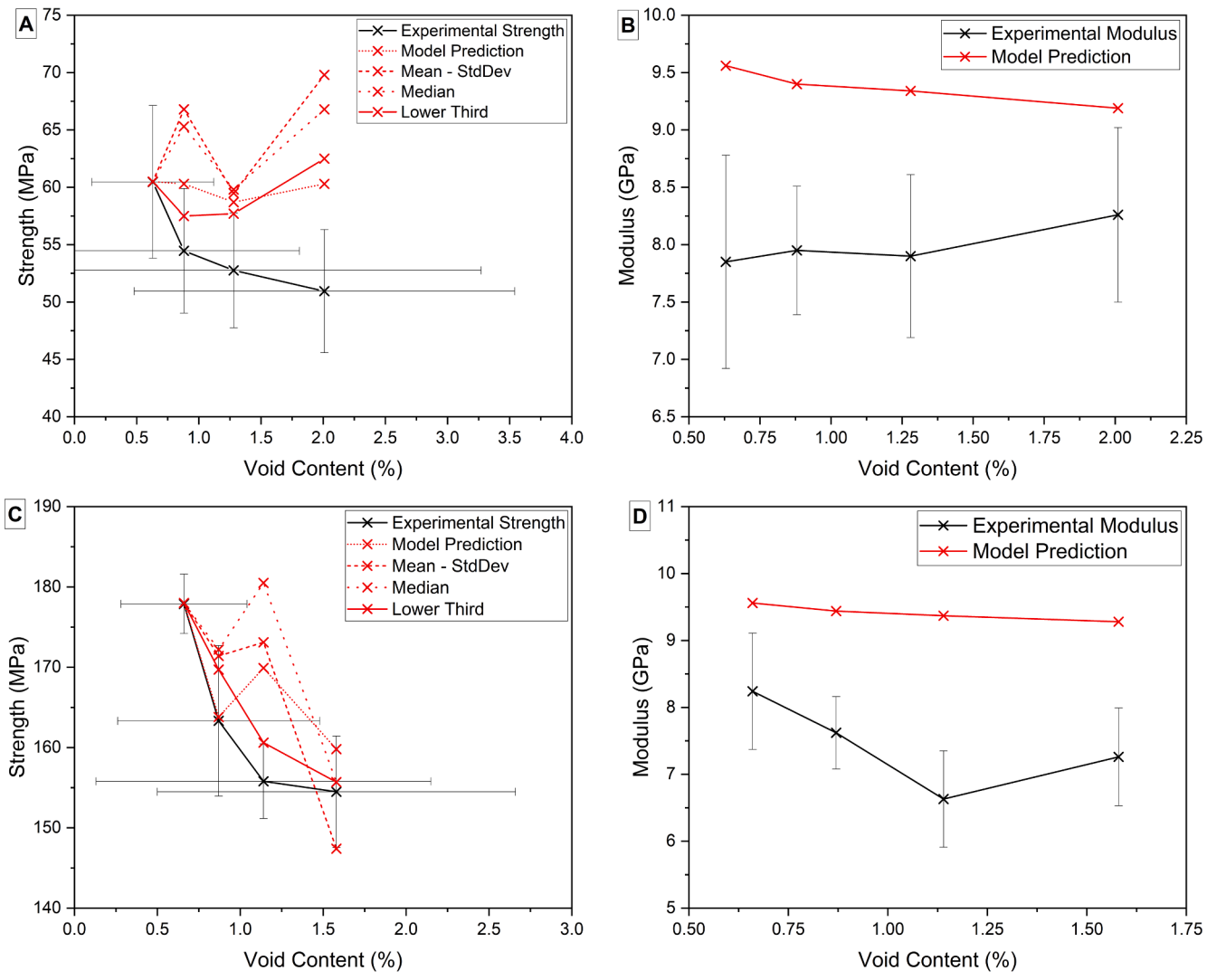

Fig. 4. Experimental Results and Model Correlation using different void characterisation techniques for (A) Tensile Strength, (B) Tensile Modulus, (C) Compressive Strength and (D) Compressive Modulus. Strength and stiffness data was calculated from the same test; therefore, the void content error is the same and has been omitted from the modulus results for clarity.

transverse strength.

4. Numerical modelling

4.1. Model conceptualisation and description

This paper presents a new approach addressing the compromise between representative geometry and computation efficiency. The approach accounts for voids in their entirety; accurate shape, size and distribution of voids are incorporated into the modelling approach whilst computational efficiency is preserved. The approach works on the assumption that porosity affects the transverse material properties, such that voids degrade the mechanical performance of the matrix. Working from this assumption a dual-stage multiscale simulation is presented. Stage 1 of the approach is the '*void module*' which predicts the impact voids have on pristine matrix; since fibres play a minimal role in the transverse direction they are excluded in this stage, significantly reducing the element count since element size is dictated by the smallest feature which would have been the fibre, however, now is the void. This results in a single homogenised phase, named the '*degraded matrix*'. The effect of the fibres is considered in the next stage where a Representative Unit Cell (RUC) using the homogenised matrix is used to predict the overall strength of the ply containing the specific voids parameters used in the first stage. The applied load in both models is increased until failure occurs, which can be calculated proportionally for a linear model or incrementally for a nonlinear model. At which point the reaction force is measured and used in combination with the cross-sectional area to calculate the homogenised strength. A schematic for the approach can be seen in Fig. 5 and details of each step are presented below.

4.2. Geometry

4.2.1. Stage 1. Void Module

The first stage in this modelling approach is to investigate how the porosity present in the laminate affects the strength of the matrix. It is at this stage where geometrical information regarding the porosity is brought into the model which accurately describes the porosity in the laminate. These parameters include void content, void distribution, and orientation as well as the shape and size of voids. Since, in practise, the microstructure is non-repeating, a representative porosity characterisation must be determined. Once the geometry of the void module is finalised the model predicts the strength of the degraded matrix. Details of model setup and homogenisation is described in Section 4.4.

4.2.2. Stage 2. Repeating unit Cell

In the transverse direction, the fibres will act as stress concentrations

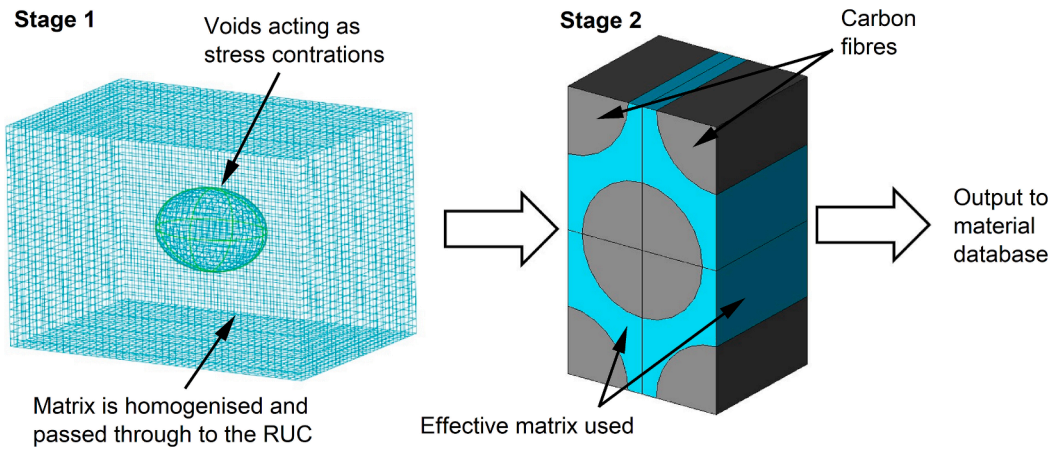

Fig. 5. Schematic of multiscale modelling approach.

and so whilst they were excluded in the first stage (to improve computational efficiency) the second stage is to evaluate the impact the fibres have on the homogenised matrix. The fibre size and distribution must also be representative of the composite. The outputs from this stage give the transverse tensile and compressive strength for a ply which contains void geometry as modelled in stage 1.

4.3. Material properties and failure criteria

Fig. 6 shows a typical stress–strain graph of a laboratory tested tensile and compressive specimen where only a minimal amount of plasticity is identified in just the compressive samples. For this reason both the void module and RUC brittle failure is assumed, in line with other literature [31–33]. This also means that only the linear elastic material properties (Young's modulus and Poisson's Ratio) are included in the model. There are several benefits to the assumption of brittle failure; firstly, computational efficiency is preserved since a linear elastic model is significantly faster to run than a nonlinear simulation. Secondly, fewer material properties are required to be input into the model which saves on costly testing if this information is not known. So, whist brittle failure is conservative, it is deemed an appropriate approach. If a user case required material plasticity, then the material properties could be changed accordingly, however, this would have an associated impact on the computational efficiency.

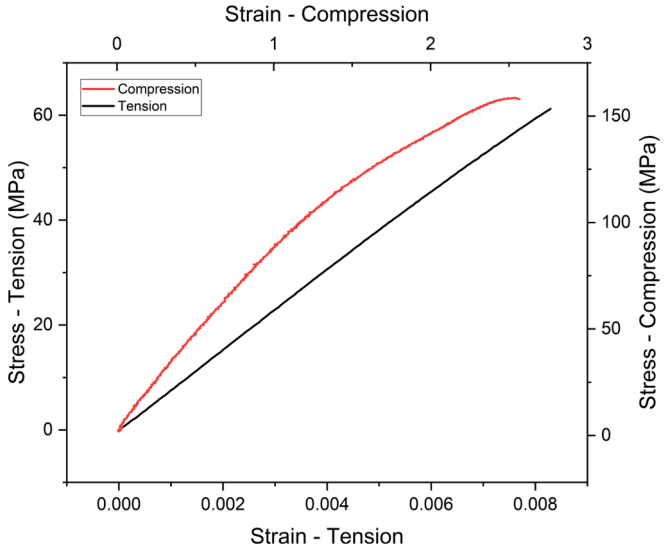

Fig. 6. Typical experimental stress–strain plots of both 90° compression and tension specimens.

To identify failure in both models, they are loaded until a single matrix element has failed using the Von Mises Failure Criterion, calculated using Equation (1), where σ_{vm} is the Von Mises stress, and σ_{ij} (ij = 11, 22, 33, 12, 23 and 13) are the stress tensor components. Failure is determined when the Von Mises stress matches the strength of the matrix at which point catastrophic failure is assumed.

$$\sigma_{vm} = 1/\sqrt{2}\sqrt{(\sigma_{11}-\sigma_{22})^2 + (\sigma_{22}-\sigma_{33})^2 + (\sigma_{33}-\sigma_{11})^2 + 6(\sigma_{23}^2 + \sigma_{31}^2 + \sigma_{12}^2)^2} \quad (1)$$

4.4. Boundary conditions and homogenisation

To constrain each model a symmetry boundary condition is used on the designated fixed face. This allows for Poisson's effect to still take place whilst preventing displacement in the loaded direction. Depending on the geometrical attributes of the voids, it may be possible to use symmetry boundary conditions and use a ½ or ¼ model to improve computational efficiency, however, this may not always be the case and is completely reliant on porosity formation. To load both the void module and RUC a displacement boundary condition is applied to the loaded surface which is opposite the constrained side. The selected constrained and loaded surfaces must be in keeping with the orientation of the voids. Periodic boundary conditions were also be applied to the RUC to simulate periodicity.

Load is increased and once an element has been identified to have failed the model is homogenised for either the matrix or ply strength (depending on which stage model is being run). This output is then used in the following stage of the modelling approach. i.e., the void module is homogenised to output the effective matrix strength to be used in the RUC which is then homogenised to be used in a design calculation at the ply/layup level. The homogenisation process works by measuring the reaction force on the constrained surface at the instance an element has failed. Once the force required for failure is known the effective strength of the model can be calculated using the cross-sectional area.

4.5. Determination of material properties

Fibre properties are usually readily available from supplier data sheets; however, matrix properties can often be more challenging to establish. Particularly in the case of pre-preg materials where suppliers commonly don't provide data on individual constituents. This is particularly challenging for this approach where knowledge of pristine matrix properties is important. To address this challenge, here an inverse modelling approach is adopted, and laminate experimental data is used to derive the matrix properties as follows. This approach only uses

a single datapoint for either tension or compression and is independent from the remaining test data. This is to say that the other results do not have any influence on how the matrix properties are derived.

Firstly, the bulk stress in the RUC is set to be equivalent to the failure strength of the laminate tested, based on the reaction forces generated in the RUC. At this instance, the maximum Von Mises stress found from any matrix element is taken to be the homogenised matrix strength of the void module. Next, the void module is used to predict the strength of the pristine matrix in a similar manner to that of the previous RUC step. A stress equivalent to the homogenised matrix strength determined from the RUC is applied to the void module, based on the reaction forces generated. Again, at this instance the maximum Von Mises stress is found and taken to be the pristine matrix strength. This approach can be used in both tension and compression provided there is the corresponding tensile or compressive experimental data available.

5. Model application

5.1. Model setup using experimental results

The characterisation results in section 3.1 are used to generate the geometry in the modelling process. A single void was modelled in the step 1 model since the microscopy showed an even distribution of voids of the same size. The overall dimensions of the void module were dictated by the size of the void and the corresponding void content, whilst keeping the aspect ratio of the module the same as that of the void. Knowing that the volume fraction of the matrix is 40% and the fibre diameters are 7 μm with a 45° spacing, assuming uniform distribution, the RUC geometry can be generated with an overall dimension of 5.19 μm^3.

A quarter model was utilised using symmetry boundary conditions to improve computational efficiency of the stage 1 model. For the stage 2 model Periodic Boundary Conditions (PBC) were used on the sides of the model to preserve periodicity. PBC were implemented used the Periodic Boundary Condition plugin for Abaqus/CAE and can be found at the Github depository [26]. Surfaces where the boundary conditions were applied can be seen as an overlay in Fig. 7.

All analyses were built using 8-node 3D linear brick elements without reduced integration (C3D8). Element size control was based on a combination of local seed control around features such as void and fibre circumference and global meshing. The element approximate size was based on the results of a mesh convergency study whereby the change in stress distribution and maximum stress was observed as element size was reduced. The appropriate element size was determined at the point where the stress distribution and maximum stress was only minimally affected.

Table 3 presents the constituent properties used in the model. Only the fibre tensile strength and modulus were made available and were taken from the manufacturer's datasheet. Therefore, the remaining properties were taken from literature. This included the Poisson's ratio for both the fibre [27,33] and matrix [27,33,34] as well as the matrix modulus [27,33]–[37]. The strength of the matrix was determined by the inverse modelling process, described in section 4.5, using the tensile and compressive laminates cured at 0.59 MPa and 0.39 MPa respectively (determined based on lowest void content). As different void characterisation approaches were used, this resulted in a range of values. The results are comparable with findings reported by Hobbiebrunken et al. [35] who reported a tensile strength of an epoxy micro-fibre (to minimize defects found in macro testing) being 135 ± 21 MPa and predicted a compressive strength of up approximately 327 MPa.

Table 3
Constituent Material Properties used in the model.

Constituent	Young's Modulus / GPa	Poisson's Ratio	Tensile Strength / MPa	Compressive Strength / MPa
Fibre	235	0.20	$4.12x10^3$	N/A
Matrix	3.0	0.35	135.7–143.2	357.9–370.5

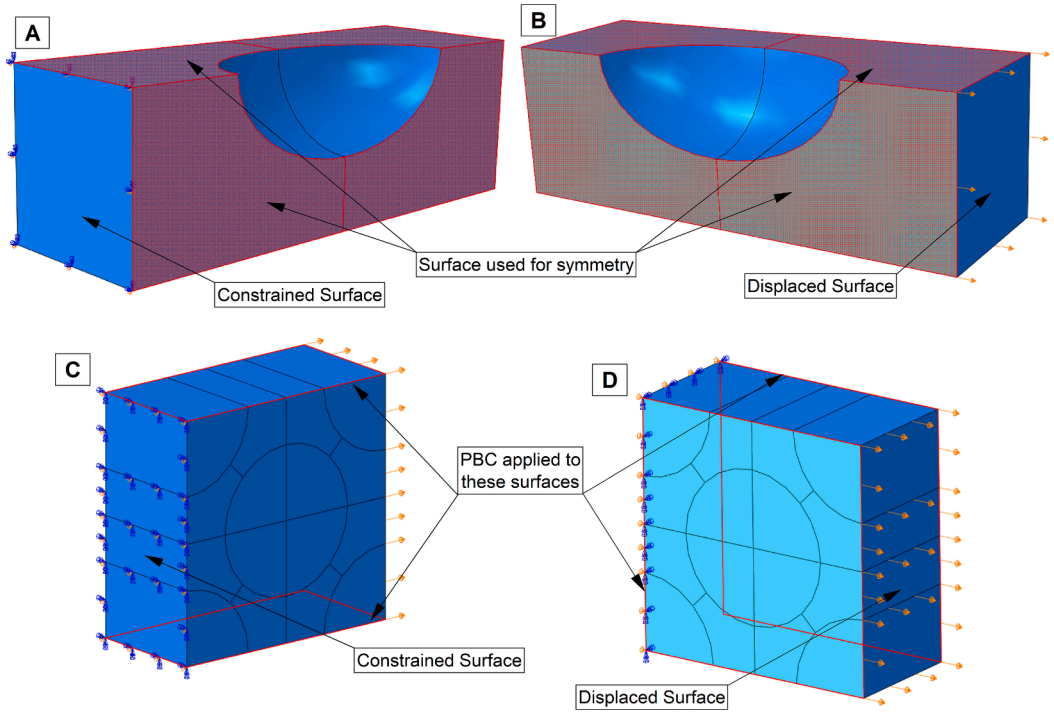

Fig. 7. Surfaces used for constraining and applying displacement to, as well as the surfaces used for applying symmetry and PBC. (A) and (B) represent the void module and (C) and (D) represent the RUC.

5.2. Simulation results and correlation

Simulations were performed using Abaqus/CAE 2019 running on an AMD Ryzen 7 3700X CPU using 6 of the available cores. The predicted transverse tensile and compressive strengths of each laminate, based on the void characterisation results, can be seen in Fig. 4(A) and (C). Depending on the void characterisation technique used resulted in a spread in the model prediction. What was found, was that the techniques that accounts for all the measurements (such as the mean of all dimensions within each dataset) have a lower correlation. This can be explained by the reasoning that within each dataset there are a few measurements of large voids (relative to the majority of the voids found in the laminate) which skew the results. By having larger measurements means that the stress concentration around the void is reduced, resulting in an overprediction in strength. Further analysis of this affect is presented in subsection 5.3. The general approach that yielded best correlation was taking the mean of the lower third number of measurements. This meant that the higher number of smaller voids, which would have the higher stress concentrations, were better represented. The only exception to this was the 0.05 MPa tensile laminate. For this laminate, it was found to have a broader spread in longitudinal lengths and so even when using the lower third resulted in an overprediction. When observing the relative frequency histogram plot for that laminate, as shown in Fig. 8, it was seen that the majority of voids had a longitudinal dimension between 15 and 30 μm and a transverse dimension of 0–45 μm. For this reason, it was determined that a spherical void of diameter 20 μm was the most representative of the smaller voids. The model was then run using the revised dimensions for the 0.05 MPa tensile laminate and the final correlation between the model prediction and the experimental strength results is shown in Fig. 9.

The final model results are overlaid against the corresponding experimental results presented in Fig. 9 and show good correlation exhibiting a similar degrative trend such that as the void content increases the strength reduces. The matrix strength derivation using the lowest void content laminates explains near perfect correlation on the respective datapoints. The remaining three data points for of the tensile models fall within 10 % of the mean test data, and within 4 % of the compressive mean test data. In almost all cases the models fall within the error bars, except for the 0.19 MPa compressive model, which only has a slight overprediction. There does appear to show a very slight increase in strength between the 0.19 MPa and 0.39 MPa models. This can be explained by the models accounting for three void characterisation variables (void content, longitudinal length, and transverse length), however, only being plotted against one variable (void content). As all three variables are different between the models means that each model will have a different correlation to the experimental data. In this case the 0.9 % void content laminate has a better correlation than that of the 1.3 % laminate.

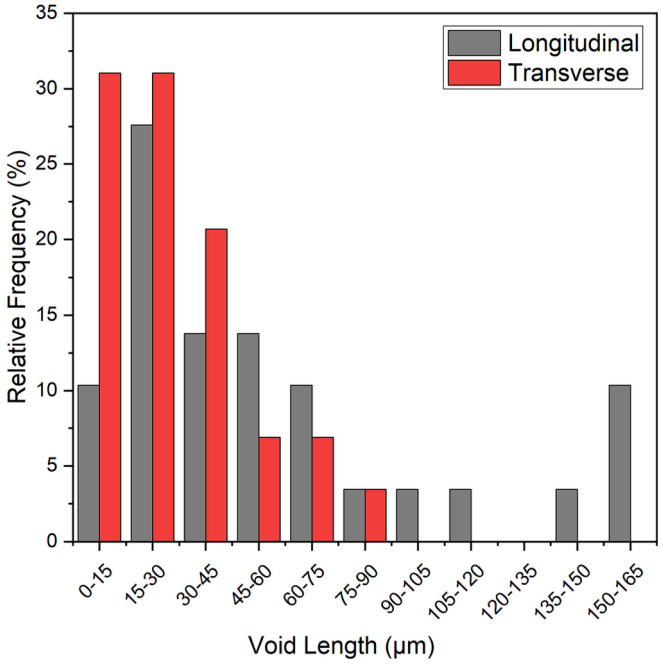

Fig. 8. Relative frequency plot of the 0.05 MPa tensile laminate, showing a broad spread in longitudinal lengths.

Another observation is that the compressive series of models followed the same non-linear trend seen from the experimental testing, whereas the tensile models predicted a more linear trend. This is likely due to a simplification of the porosity being assumed as a single representative void and the complete porosity parameters across the samples are not captured. This simplification also explains the over prediction of the model as small microvoids with high stress concentrations are not modelled explicitly, and as shown in subsection 5.3, these have a lower load to failure. In practise voids generate in a number of shapes and sizes, and whilst it is near impossible to accurately describe them completely, a compromise between accuracy and representative geometry must be made. This process considers not only the void content attribute but also geometry. However, porosity characterisation through microscopy has its limitations such as measurements limited to 2 dimensions, difficulty in accurately measuring the smallest voids and number of voids measured limited due to extensive input required. It is likely that the difficulty in measuring the smallest of voids (which act as sharp stress raisers) and voids having more complex geometry around the fibres than a simple ellipsoid contributes to the over prediction.

Although the modulus was not the focus of the study, it could also be measured and compared to the experimental results, as shown in Fig. 4 (B) and (D). As found from the experimental testing, there is only a very slight reduction in stiffness as the void content increases. The model has an over prediction in modulus for both tensile and compressive models and this is likely due to using literature to estimate the modulus of pristine matrix.

Overall, however, the results show that by considering both void geometry as well as void content, the model correlates well with laboratory tests. In tension all models fall within experimental error and whilst only one of the compressive models fell very slightly outside of the error range, they are all still within 4%. One of the main benefits of this approach is the speed that the simulations take to run. High computational power is often associated with micromechanical studies [36,37], however, as shown in Table 4, whilst the models have got element numbers in the 10′s of thousands, the longest simulation took just over two minutes. This demonstrates the efficiency and speed at which models can be iterated through. The main contribution to the minimal simulation time is that the models were linear elastic. It is acknowledged that if plasticity were to be included in a non-linear analysis, then the simulation time would increase accordingly. What is presented in this paper is a framework for analysis and by having an efficient process means that there is scope to develop the void characterisation and implementation of more complex geometry and material definition without high penalties in computational cost.

5.3. Void shape influence

An observation was made from the experimental analysis that there was a non-linear trend such that as porosity increased there was a reduction in the rate at which strength was affected. This was determined as a result of an increase in size, specifically longitudinal length, of the voids at higher void contents. This effect was simulated using the Stage 1 model. The void content was kept constant at 1.0 % and the transverse length was fixed to 5 μm. By increasing the length of the longitudinal axis from 2.5 μm up to 20 μm the strength of the Stage 1 model increases, illustrated in Fig. 10. This demonstrates that whilst

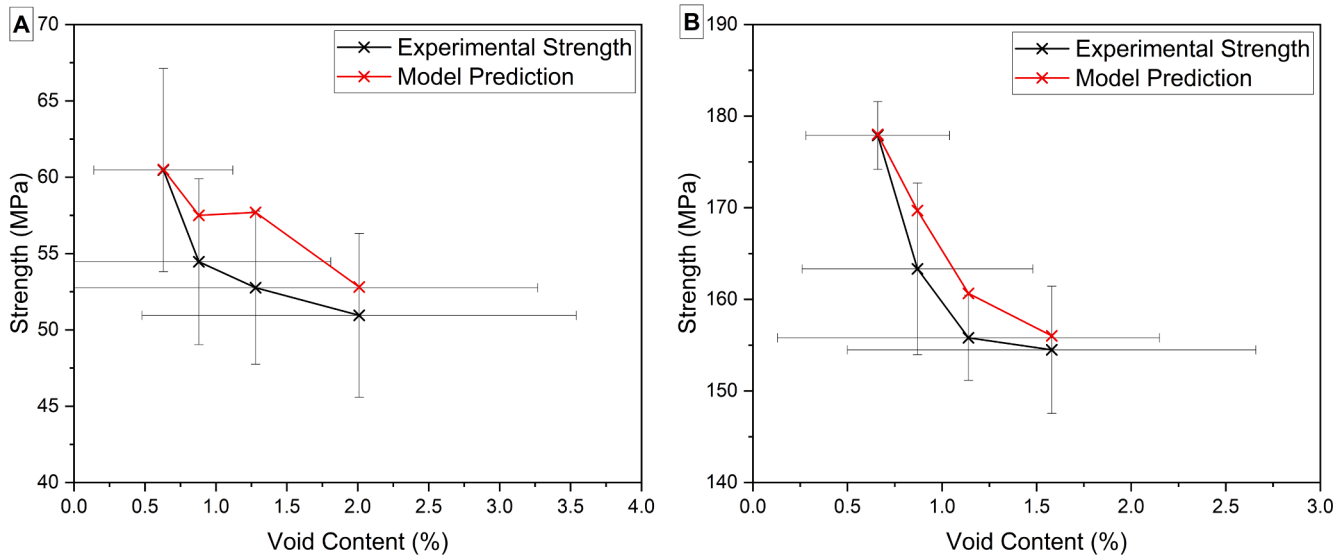

Fig. 9. Correlation between model prediction and experimental strength for (A) tension and (B) compression.

Table 4
Element number and simulation times for each model.

Model	Stage 1 - Tension				Stage 1 - Compression				Stage 2
	0.59 MPa	0.39 MPa	0.19 MPa	0.05 MPa	0.59 MPa	0.39 MPa	0.19 MPa	0.05 MPa	RUC
Element count	165,472	119,248	41,648	57,296	83,966	51,030	71,398	112,328	9,581
Simulation time / s	129	97	49	56	61	44	54	82	111

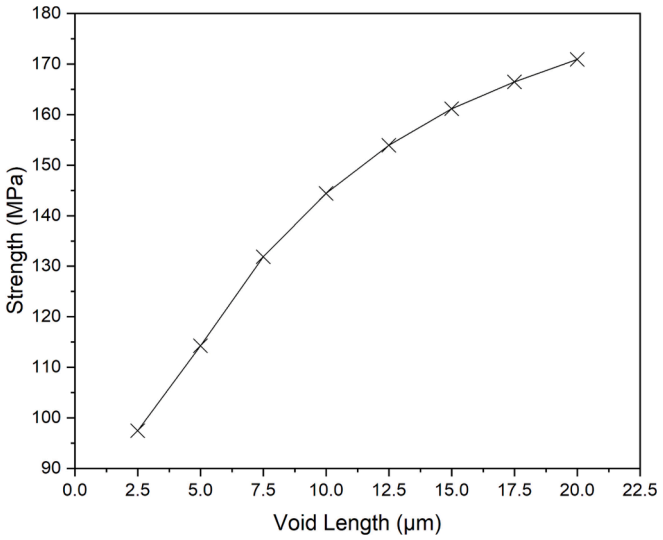

Fig. 10. Influence of void length on the strength of the Stage 1 model.

increasing the void content reduces the overall strength, the impact is lessened since the stress concentration surrounding the voids is reduced. This further demonstrates the importance of considering both geometrical parameters as well as the void content. This also helps to explain why certain approaches used to represent void geometry overestimate the strength when several larger more elongated voids are included.

Conclusions

Understanding how manufacturing induced defects, in particular porosity, affects the mechanical performance in structural composites is vitally important. If not properly assessed then either the structure will fail prematurely if porosity is not accounted for, or high safety factors will over engineer and add excess mass to the structure. The extent to which porosity affects the mechanical performance has been demonstrated by the research presented here as the results show that even by only a small increase in void content both the transverse tensile and compressive strength is significantly compromised.

To address this issue a novel multiscale modelling approach has been developed and is presented here which can account for accurate porosity generation within a laminate/component and in turn is able to predict the degradation in transverse strength. The output of the modelling approach is the accurate material properties for a given porosity generation which can be used in a manufacturing or component design study. The modelling approach has been experimentally validated using porosity characterisation of the specimens tested, to generate accurate models of each laminate and a very good correlation between the experimental data and predicted strengths has been shown.

Funding

This research did not receive any specific grant from funding agencies in the public, commercial, or not-for-profit sectors.

Data Availability

The raw/processed data required to reproduce these findings cannot be shared at this time as the data also forms part of an ongoing study.

CRediT authorship contribution statement

Benjamin Fisher: Conceptualization, Methodology, Formal analysis, Investigation, Writing – original draft, Writing – review & editing. **Mark Eaton:** Formal analysis, Writing – review & editing, Supervision. **Rhys Pullin:** Formal analysis, Writing – review & editing, Supervision.

Declaration of Competing Interest

The authors declare that they have no known competing financial interests or personal relationships that could have appeared to influence the work reported in this paper.

Data availability

Data will be made available on request.

References

[1] Leach F, Kalghatgi G, Stone R, Miles P. The scope for improving the efficiency and environmental impact of internal combustion engines. Transp Eng Jun. 2020;1:100005. https://doi.org/10.1016/j.treng.2020.100005.

[2] Kalghatgi G. Is it really the end of internal combustion engines and petroleum in transport? Appl Energy Sep. 2018;225:965–74. https://doi.org/10.1016/j.apenergy.2018.05.076.

[3] Datye AK, Votsmeier M. Opportunities and challenges in the development of advanced materials for emission control catalysts. Nat Mater Aug. 2021;20(8):1049–59. https://doi.org/10.1038/s41563-020-00805-3.

[4] Liu Q, Lin Y, Zong Z, Sun G, Li Q. Lightweight design of carbon twill weave fabric composite body structure for electric vehicle. Compos Struct Mar. 2013;97:231–8. https://doi.org/10.1016/j.compstruct.2012.09.052.

[5] Ishikawa T, et al. Overview of automotive structural composites technology developments in Japan. Compos Sci Technol Feb. 2018;155:221–46. https://doi.org/10.1016/j.compscitech.2017.09.015.

[6] Kim D-H, Kim H-G, Kim H-S. Design optimization and manufacture of hybrid glass/carbon fiber reinforced composite bumper beam for automobile vehicle. Compos Struct Nov. 2015;131:742–52. https://doi.org/10.1016/j.compstruct.2015.06.028.

[7] Potter K, Khan B, Wisnom M, Bell T, Stevens J. Variability, fibre waviness and misalignment in the determination of the properties of composite materials and structures. Compos Part Appl Sci Manuf Sep. 2008;39(9):1343–54. https://doi.org/10.1016/j.compositesa.2008.04.016.

[8] Kalantari M, Dong C, Davies IJ. Effect of matrix voids, fibre misalignment and thickness variation on multi-objective robust optimization of carbon/glass fibre-reinforced hybrid composites under flexural loading. Compos Part B Eng Aug. 2017;123:136–47. https://doi.org/10.1016/j.compositesb.2017.05.022.

[9] Mukherjee S, Ganguli R, Gopalakrishnan S. Optimization of laminated composite structure considering uncertainty effects. Mech Adv Mater Struct Mar. 2019;26(6):493–502. https://doi.org/10.1080/15376494.2017.1400621.

[10] Mesogitis TS, Skordos AA, Long AC. Uncertainty in the manufacturing of fibrous thermosetting composites: A review. Compos Part Appl Sci Manuf Feb. 2014;57:67–75. https://doi.org/10.1016/j.compositesa.2013.11.004.

[11] Zhou K, Enos R, Zhang D, Tang J. Uncertainty analysis of curing-induced dimensional variability of composite structures utilizing physics-guided Gaussian process meta-modeling. Compos Struct Jan. 2022;280:114816. https://doi.org/10.1016/j.compstruct.2021.114816.

[12] Olivier P, Cottu JP, Ferret B. Effects of cure cycle pressure and voids on some mechanical properties of carbon/epoxy laminates. Composites Jul. 1995;26(7):509–15. https://doi.org/10.1016/0010-4361(95)96808-J.

[13] Zhang A, Lu H, Zhang D. Effects of voids on residual tensile strength after impact of hygrothermal conditioned CFRP laminates. Compos Struct Jan. 2013;95:322–7. https://doi.org/10.1016/j.compstruct.2012.08.001.

[14] Li SJ, et al. The influence of cure pressure on microstructure, temperature field and mechanical properties of advanced polymer-matrix composite laminates. Fibers Polym Nov. 2014;15(11):2404–9. https://doi.org/10.1007/s12221-014-2404-0.

[15] Stamopoulos A, Tserpes K, Prucha P, Vavrik D. Evaluation of porosity effects on the mechanical properties of carbon fiber-reinforced plastic unidirectional laminates by X-ray computed tomography and mechanical testing. J Compos Mater Jun. 2016;50(15):2087–98. https://doi.org/10.1177/0021998315602049.

[16] Liu L, Zhang B-M, Wang D-F, Wu Z-J. Effects of cure cycles on void content and mechanical properties of composite laminates. Compos Struct Jun. 2006;73(3):303–9. https://doi.org/10.1016/j.compstruct.2005.02.001.

[17] Costa ML, de Almeida SFM, Rezende MC. The influence of porosity on the interlaminar shear strength of carbon/epoxy and carbon/bismaleimide fabric laminates. Compos Sci Technol Nov. 2001;61(14):2101–8. https://doi.org/10.1016/S0266-3538(01)00157-9.

[18] Di Landro L, Montalto A, Bettini P, Guerra S, Montagnoli F, Rigamonti M. Detection of Voids in Carbon/Epoxy Laminates and Their Influence on Mechanical Properties. Polym Polym Compos Jun. 2017;25(5):371–80. https://doi.org/10.1177/096739111702500506.

[19] Nikopour H. A virtual frame work for predication of effect of voids on transverse elasticity of a unidirectionally reinforced composite. Comput Mater Sci Nov. 2013;79:25–30. https://doi.org/10.1016/j.commatsci.2013.05.049.

[20] Dong C. Effects of Process-Induced Voids on the Properties of Fibre Reinforced Composites. J Mater Sci Technol Jul. 2016;32(7):597–604. https://doi.org/10.1016/j.jmst.2016.04.011.

[21] Li B, Zhao M, Wan X. The influence of void distribution on transverse mechanical properties of unidirectional composites. In: 2017 8th International Conference on Mechanical and Aerospace Engineering (ICMAE), Prague, Czech Republic, Jul. 2017, pp. 209–214. https://doi.org/10.1109/ICMAE.2017.8038644.

[22] Ashouri Vajari D, González C, Llorca J, Legarth BN. A numerical study of the influence of microvoids in the transverse mechanical response of unidirectional composites. Compos Sci Technol Jun. 2014;97:46–54. https://doi.org/10.1016/j.compscitech.2014.04.004.

[23] Huang T, Gong Y. A multiscale analysis for predicting the elastic properties of 3D woven composites containing void defects. Compos Struct Feb. 2018;185:401–10. https://doi.org/10.1016/j.compstruct.2017.11.046.

[24] Dong J, Huo N. A two-scale method for predicting the mechanical properties of 3D braided composites with internal defects. Compos Struct Sep. 2016;152:1–10. https://doi.org/10.1016/j.compstruct.2016.05.025.

[25] Jiang H, Ren Y, Liu Z, Zhang S. Microscale finite element analysis for predicting effects of air voids on mechanical properties of single fiber bundle in composites. J Mater Sci Jan. 2019;54(2):1363–81. https://doi.org/10.1007/s10853-018-2928-6.

[26] 'GitHub - smrg-uob/PeriodicBoundaryCondition: A plugin for Abaqus CAE 2018 to define periodic boundary conditions to 3D geometry', *GitHub*. https://github.com/smrg-uob/PeriodicBoundaryCondition (accessed Jun. 28, 2022).

[27] Yang L, Yan Y, Ran Z, Liu Y. A new method for generating random fibre distributions for fibre reinforced composites. Compos Sci Technol Mar. 2013;76:14–20. https://doi.org/10.1016/j.compscitech.2012.12.001.

[28] Mehdikhani M, Petrov NA, Straumit I, Melro AR, Lomov SV, Gorbatikh L. The effect of voids on matrix cracking in composite laminates as revealed by combined computations at the micro- and meso-scales. Compos Part Appl Sci Manuf Feb. 2019;117:180–92. https://doi.org/10.1016/j.compositesa.2018.11.009.

[29] Huang H, Talreja R. Effects of void geometry on elastic properties of unidirectional fiber reinforced composites. Compos Sci Technol Oct. 2005;65(13):1964–81. https://doi.org/10.1016/j.compscitech.2005.02.019.

[30] van de Werken N, Koirala P, Ghorbani J, Doyle D, Tehrani M. Investigating the hot isostatic pressing of an additively manufactured continuous carbon fiber reinforced PEEK composite. Addit Manuf Jan. 2021;37:101634. https://doi.org/10.1016/j.addma.2020.101634.

[31] Sebaey TA, Bouhrara M, O'Dowd N. Fibre Alignment and Void Assessment in Thermoplastic Carbon Fibre Reinforced Polymers Manufactured by Automated Tape Placement. Polymers Feb. 2021;13(3):473. https://doi.org/10.3390/polym13030473.

[32] Rouf K, Worswick MJ, Montesano J. A multiscale framework for predicting the mechanical properties of unidirectional non-crimp fabric composites with manufacturing induced defects. J Compos Mater Mar. 2021;55(6):741–57. https://doi.org/10.1177/0021998320958189.

[33] Marklund E, Asp LE, Olsson R. Transverse strength of unidirectional non-crimp fabric composites: Multiscale modelling. Compos Part B Eng Oct. 2014;65:47–56. https://doi.org/10.1016/j.compositesb.2014.01.053.

[34] Chevalier J, Morelle XP, Bailly C, Camanho PP, Pardoen T, Lani F. Micro-mechanics based pressure dependent failure model for highly cross-linked epoxy resins. Eng Fract Mech Jun. 2016;158:1–12. https://doi.org/10.1016/j.engfracmech.2016.02.039.

[35] Hobbiebrunken T, Fiedler B, Hojo M, Tanaka M. Experimental determination of the true epoxy resin strength using micro-scaled specimens. Compos Part Appl Sci Manuf Mar. 2007;38(3):814–8. https://doi.org/10.1016/j.compositesa.2006.08.006.

[36] Mehdikhani M, Gorbatikh L, Verpoest I, Lomov SV. Voids in fiber-reinforced polymer composites: A review on their formation, characteristics, and effects on mechanical performance. J Compos Mater May 2019;53(12):1579–669. https://doi.org/10.1177/0021998318772152.

[37] Carrera E, Petrolo M, Nagaraj MH, Delicata M. Evaluation of the influence of voids on 3D representative volume elements of fiber-reinforced polymer composites using CUF micromechanics. Compos Struct 2020;254:15. https://doi.org/10.1016/j.compstruct.2020.112833.